Published in partnership with CECCR at King Abdulaziz University



https://doi.org/10.1038/s41612-025-01004-0

# Understanding the driving mechanisms behind triple-dip La Niñas: insights from the prediction perspective

Check for updates

Han-Ching Chen¹,² ⋈, Yu-Heng Tseng³,⁴ ⋈, Jo-Hsu Huang³ & Ping-Han Juang³

This study investigates the mechanisms and predictability of multi-year La Niña events, focusing on the 1998–2001 and 2020–2023 triple-dip events, using a physically based statistical ENSO prediction model (EPM). The results highlight distinct driving mechanisms behind these two events. The 1998–2001 event was primarily initiated by substantial negative heat content anomalies in the equatorial Pacific, which resulted from the preceding strong El Niño. These negative heat content anomalies played a crucial role in sustaining cold sea surface temperature anomalies (SSTA) into the third year. In contrast, the 2020–2023 event, which lacked significant negative heat content anomalies, was characterized by persistent equatorial easterly wind anomalies induced by extratropical forcing from the Southern Hemisphere. The EPM successfully captures these differences, with tropical ocean-atmosphere coupling being the dominant factor in predictability for 1998–2001, especially during the second year, whereas extratropical forcing played a key role in improving forecasts for 2020–2023. These findings highlight the importance of incorporating extratropical influences to enhance the prediction skill of multi-year La Niña events, especially those with atypical tropical precursors.

With the anticipated increase of occurrence in the future climate, the La Niña phenomenon has received widespread attention as a crucial climate event. La Niña is part of the El Niño-Southern Oscillation (ENSO) cycle, characterized by quasi-periodic variations in sea surface temperatures (SST) in the equatorial Pacific. Unlike El Niño events, La Niña events are typically long-lasting, often extending into a second or even third year, known as double-dip or triple-dip events, with more prolonged global impacts<sup>1-3</sup>. Research suggested that under global warming, the frequency of multi-year La Niña events increases significantly<sup>4,5</sup>. However, understanding and predicting multi-year La Niña events, especially triple-dip La Niña, presents greater challenges than predicting single-year El Niño or La Niña events. This complexity arises from the intricate interactions between the ocean and atmosphere, involving not only tropical dynamics but also extratropical forcing<sup>6-10</sup>. Furthermore, triple-dip La Niña events have been exceedingly rare during the period of reliable observational data after 1980, with occurrences observed only in 1998-2001 and 2020-2023, making them difficult to study.

Some studies have demonstrated that the asymmetry of ENSO-related tropical ocean-atmosphere processes can explain why La Niña events often persist much longer than El Niño events. A prevailing hypothesis for several multi-year La Niña events is that they occur following strong El Niño events, which provide sufficient cold anomalies of heat content through a significant discharge process to sustain subsequent multi-year La Niña events<sup>11,12</sup>. Additionally, Hu et al. (2014)<sup>13</sup> argued that the off-equator cold anomalies in heat content, associated with reflected upwelling Rossby waves, may not be conducive to the equatorial recharge of upper heat content, thereby favoring the persistence of cold ocean subsurface conditions<sup>13</sup>. Iwakiri & Watanabe (2022) also proposed that a meridionally broad structure of ENSO during the decaying phase helps prevent the southward shift of the equatorial zonal wind<sup>14</sup>, contributing to the prolonged persistence of ENSO<sup>15</sup>. Consequently, the asymmetry in the meridional scale of SST anomalies (SSTA) between El Niño and La Niña 16 leads to multi-year La Niña events occurring more frequently than multi-year El Niño events. However, for an El Niño event, if the warm heat content anomalies are

¹State Key Laboratory of Climate System Prediction and Risk Management/Key Laboratory of Meteorological Disaster, Ministry of Education/Collaborative Innovation Center on Forecast and Evaluation of Meteorological Disasters, Nanjing University of Information Science and Technology, Nanjing, China. ²School of Atmospheric Sciences, Nanjing University of Information Science and Technology, Nanjing, China. ³Institute of Oceanography, National Taiwan University, Taipei, Taiwan. △Ocean Center, National Taiwan University, Taiwan. △e-mail: hanching@nuist.edu.cn; tsengyh@ntu.edu.tw

sufficiently large, and the subsurface warm anomalies are effectively maintained, the likelihood of a multi-year El Niño may increase <sup>17</sup>.

Besides tropical mechanisms, extratropical forcing is also considered to contribute to multi-year ENSO events. For example, Yu & Fang (2018)<sup>6</sup> found that the duration of ENSO events, primarily influenced by the Seasonal Footprinting Mechanisms (SFM) associated with North Pacific Oscillation (NPO)<sup>18</sup>, tends to last longer than events dominated only by the recharge-discharge process<sup>19</sup> in the tropical Pacific. Several previous studies also reported the links between multi-year ENSO and North Pacific Meridional Mode (NPMM)<sup>20</sup>, suggesting that multi-year ENSO can be forced by the North Pacific atmospheric variability<sup>7,8,21-26</sup>. Fan et al. (2023)<sup>24</sup> even found that the NPMM, when triggered by tropical forcing, tends to enhance the persistence of La Niña events more than that of El Niño events. In addition to the extratropical forcing from the North Pacific, some studies have mentioned the role of tropical-extratropical interactions from the South Pacific in initiating the multi-year La Niña event. Shi et al. (2023)<sup>27</sup> suggested that the combined effect of NPMM and South Pacific Meridional Mode (SPMM)<sup>28</sup> plays a crucial role in the recurrence of the La Niña event from 2020 to 2023.

Most existing research on multi-year La Niña relies on statistical analyses of observations/climate-model datasets or coupled general circulation model (CGCM) simulations with idealized forcing. In this study, we explore and validate the dynamical mechanisms and predictability of consecutive La Niña events using a physically based statistical ENSO prediction model (EPM)<sup>29-31</sup>. The unique innovation of this study is the use of the EPM to address these issues from a prediction perspective, considering both tropical ocean-atmosphere coupling and extratropical processes in the Pacific Ocean. This approach allows us to examine the relative contributions of various processes to consecutive La Niña events. By enhancing our understanding of the formation of double- or triple-dip La Niña events and the associated dynamic processes, this study ultimately improves the accuracy of climate models and our ability to forecast ENSO events.

#### Results

#### Characteristics of multi-year La Niña

Figure 1 shows the 3-month running averaged Niño3.4 index based on ERSSTv5 between 1980 and 2023 for El Niño and La Niña events. The composite El Niño and La Niña evolution (thick black lines) typically exhibits an onset during spring, followed by rapid growth throughout summer, peaking in winter, and subsequent decay in the following year. Hereafter, the seasonality refers to the Northern Hemisphere. Most El Niño events turn to negative SSTA by the spring of the following year, often evolving into La Niña conditions (Fig. 1a). However, La Niña events

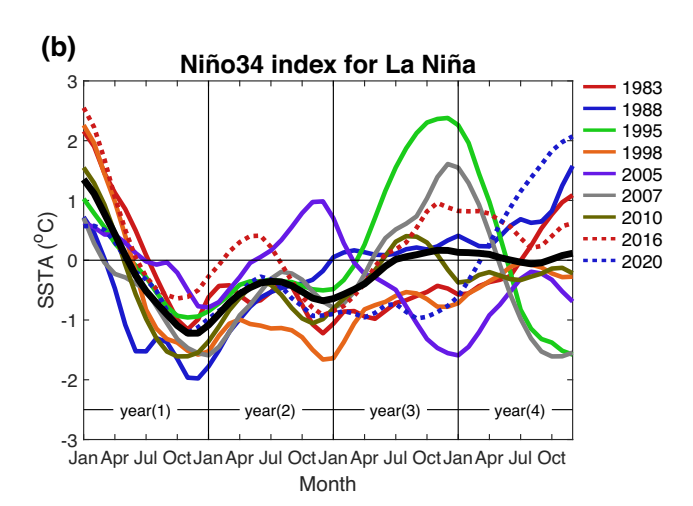
(a) Niño34 index for El Niño 3 1982 1986 1991 2 1994 1997 2002 2004 SSTA (°C) 2006 2009 2014 2018 -1 -2 year(2) year(3) Jan Apr Jul Oct Jan Apr Jul Oct Jan Apr Jul Oct Jan Apr Jul Oct Month

**Fig. 1** | **SSTA evolution during El Niño and La Niña events.** The 3-month running average of Niño3.4 index based on ERSSTv5 from 1980 to 2023 for **(a)** El Niño and **(b)** La Niña events. For multi-year events only the first event is selected to avoid

frequently show multi-year persistence, with decaying negative SSTA reintensifying during the summer of the second year and peaking again in the following winter (Fig. 1b). In particular, the La Niña events of 1998 and 2020 persisted for three consecutive years. These results suggest an asymmetry: while El Niño tends to occur as a single-year phenomenon, La Niña is more likely to multi-year recurrence. Although extensive literature discusses La Niña's persistence into a second year, the forecast skill of major forecasting centers in predicting multi-year La Niña events remains limited, as evidenced by the IRI/CPC plume predictions for the recent 2020-2023 tripledip La Niña event (Fig. 2). Most models failed to successfully predict the occurrence of the second La Niña from April 2021. Moreover, research on triple-dip La Niña events remains sparse. Therefore, this study provides an in-depth analysis of the triple-dip La Niña events from 1998 to 2001 (comprising the 1998-1999, 1999-2000, and 2000-2001 events) and from 2020 to 2023 (comprising the 2020-2021, 2021-2022, and 2022-2023 events), aiming to improve understanding of their driving mechanisms and

In most El Niño events, zonal wind anomalies in the tropical Pacific weaken after the first winter and vanish by late spring of the second year (Fig. 3a; individual events are shown in Supplementary Fig. 1). In the absence of persistent zonal wind anomalies during this period, oppositephase thermocline anomalies (D20, depth of 20 °C isotherm) in the western Pacific can propagate as coupled oceanic Kelvin waves into the centraleastern Pacific (Fig. 3d; individual events are shown in Supplementary Figure 2), accelerating the decline of central-eastern Pacific SSTA. Similarly, in single-year La Niña events (e.g., the 1988-1999 and 2005-2006 La Niña events; Fig. 3c, f), zonal wind anomalies rapidly diminish during the first winter and disappear by the following spring, coinciding with the emergence of opposite-phase thermocline anomalies in the central-eastern Pacific. In most La Niña events (Fig. 3b, e), although SST, D20, and zonal wind anomalies can persist into the following year, the zonal wind anomalies experience a rapid decline and disappearance after the winter of the second year, causing a phase transition of SSTA during the summer of the third year.

However, for the La Niña events that began in 1998 and 2020, there are notable differences in the evolution and coupling of SSTA with zonal wind anomalies compared to most La Niña events (Fig. 4a). The case of the 1998–2001 triple-dip La Niña, followed a very strong 1997–1998 El Niño, leading to the production of sufficiently negative heat content anomalies through a significant discharge process (Fig. 4c). These cold anomalies played a critical role in counteracting the decaying processes<sup>32</sup>, sustaining the cold SSTA until the end of the third year. In contrast, the 2020–2023 triple-dip La Niña, unlike the 1998–2001 one, lacked a preceding substantial



double counting. The thick black line represents the average of all events, while the other lines represent individual ENSO events.

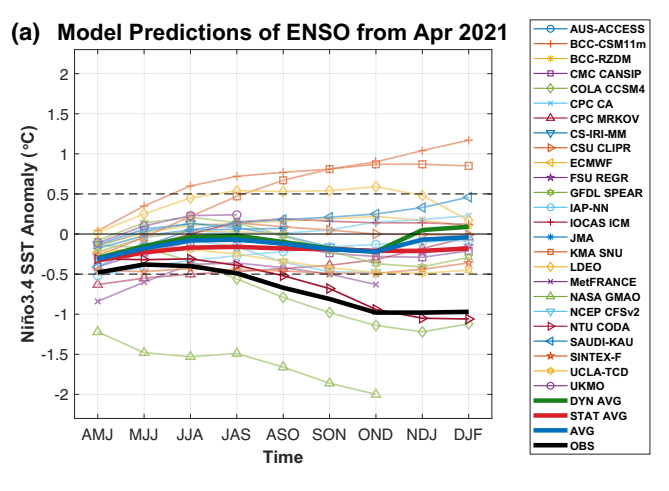
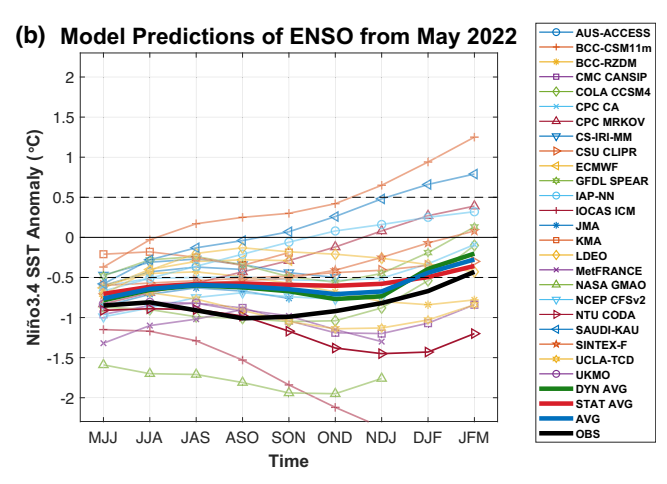


Fig. 2 | Model predictions of ENSO from spring 2021 and 2022. This figure presents ENSO forecasts from (a) April 2021 and (b) May 2022 generated by dynamical and statistical models for SSTA in the Niño3.4 region (thin lines). The green, red, and blue thick lines represent the average of dynamical models, statistical



models, and all models, respectively. The black thick line indicates the observations. The prediction data were provided by the International Research Institute for Climate and Society, Columbia University Climate School (https://iri.columbia.edu/ENSO).

El Niño and discharge process, resulting in weak negative heat content anomalies during its evolution (Fig. 4d). Nonetheless, persistent and strong easterly anomalies provide a crucial role in maintaining the cold SSTA into the end of the third year (Fig. 4b). These quasi-stationary zonal wind anomalies over the central Pacific acted as a barrier, resisting the propagation of opposite-phase thermocline anomalies from the western to the eastern Pacific (Fig. 4d). This prevented the phase transition of the SSTA and led to the three-year consecutive La Niña events. While easterly wind anomalies were observed in the spring and summer of the second and third years in both 1998-2001 and 2020-2023 triple-dip La Niña events, their origins significantly differ. ENSO-related zonal wind anomalies are typically proportional to the zonal gradient of Pacific SSTA<sup>19,33</sup>. However, despite weaker SSTA during the 2020-2023 event compared to the 1998-2001 event, stronger easterly anomalies were observed (Fig. 4a, b). This suggests that, during the 1998-2001 event, the easterly anomalies were primarily a response to the cold equatorial SSTA in the eastern Pacific. In contrast, the stronger easterly wind anomalies during the 2020-2023 event could not have been generated solely by tropical air-sea coupling processes and were likely influenced by additional mechanisms.

These results highlight the importance of heat content preconditions and their coupling with zonal wind anomalies in the development of multi-year La Niña events. For the 2020–2023 La Niña event, the lack of favorable negative heat content might have contributed to the challenges faced by many ENSO prediction models in accurately predicting the second and third years of La Niña in the springs of 2021 and 2022 (Fig. 2). In contrast, by further taking the impacts of extratropical forcing into account, the EPM described in Section "ENSO prediction model" successfully predicts subsequent La Niña events even in the absence of significant negative heat content (as shown later in Section "Prediction skill of EPM for 1998–2001 and 2020–2023 La Niña events"). This suggests a potential linkage between persistent easterly anomalies in the equatorial central Pacific and extratropical forcing.

# Evolution of 1998-2001 and 2020-2023 La Niña

To investigate the differences between the evolution of 1998–2001 and 2020–2023 events and to identify the origin of the persistent zonal wind anomalies during the 2020–2023 period, Figs. 5, 6 present the evolution of SST, D20, surface wind, and sea level pressure (SLP) anomalies for the second and third years of both events. As discussed in the previous section, the 1998–2001 La Niña was characterized by substantial negative heat content anomalies in the central-eastern Pacific (Fig. 5a–h). The large magnitude of these negative heat content anomalies resisted the decay processes typically associated with the easterly wind-induced recharge,

preventing the depletion of pre-existing negative heat content anomalies. This allowed the cold SSTA and easterly wind anomalies to persist without dissipating through the following spring and summer (Fig. 6a–h). In addition, the persistent easterly wind anomalies in the central Pacific prevented the eastward propagation of the opposite-phase heat content anomalies. As a result, the cold SSTA during this event persisted into the third year until the accumulated negative heat content anomalies were fully exhausted.

In addition to the equatorial air-sea coupling processes, extratropical forcing also contributes to the maintenance of easterly winds and cold SSTA. In the spring of 1999 (Fig. 6a), a significant north-south dipole pattern of the SLP anomalies (SLPA) was observed in the North Pacific, characteristic of the typical negative phase of the NPO mode. The southern lobe of this negative NPO induced northeasterly surface wind anomalies that strengthened the subtropical trade winds, increased the upward latent heat flux, and subsequently generated negative SSTA, known as the negative NPMM. The anomalous northeasterly associated with the NPMM not only contributed to the development of anomalous easterlies near the equator but also drove poleward upper ocean mass transport via the "trade wind charging" mechanism<sup>34-37</sup>, thereby strengthening or sustaining the cold SSTA in the equatorial Pacific. In the spring of 2000, in addition to the North Pacific forcing, the South Pacific also exhibited an SLPA dipole, located between subtropical and higher latitudes with a nodal point near 50°S (Fig. 6e). This dipole, characteristic of the negative phase of the SPMM, generated high-pressure anomalies in the southern extratropical Pacific (20°S-50°S). The associated anti-cyclonic wind anomalies induced southeasterly winds near the equator in the South Pacific, contributing to the maintenance of equatorial easterly zonal wind anomalies. However, in this event, the connection between these extratropical winds and equatorial easterlies appeared relatively localized and less continuous.

On the other hand, the 2020–2023 La Niña lacked significant negative heat content anomalies (Fig. 5i–p) due to the absence of a preceding substantial El Niño and its associated discharge process. Despite these insufficient ocean heat content conditions, persistent strong easterly zonal wind anomalies prevailed along the equator for three consecutive years (Fig. 6i–p), serving as the primary forcing that sustained the cold SSTA throughout the event. This persistence of easterly anomalies was closely linked to extratropical atmospheric forcing. A pronounced meridional SLPA dipole, centered around 50°S, developed during 2021 JJA/SON and 2022 MAM/JJA, exhibiting strong high-pressure anomalies over the southern extratropical Pacific (20°S–50°S). The associated anti-cyclonic wind anomalies formed a coherent and continuous connection with the equatorial easterly winds, effectively bridging the Southern Hemisphere and

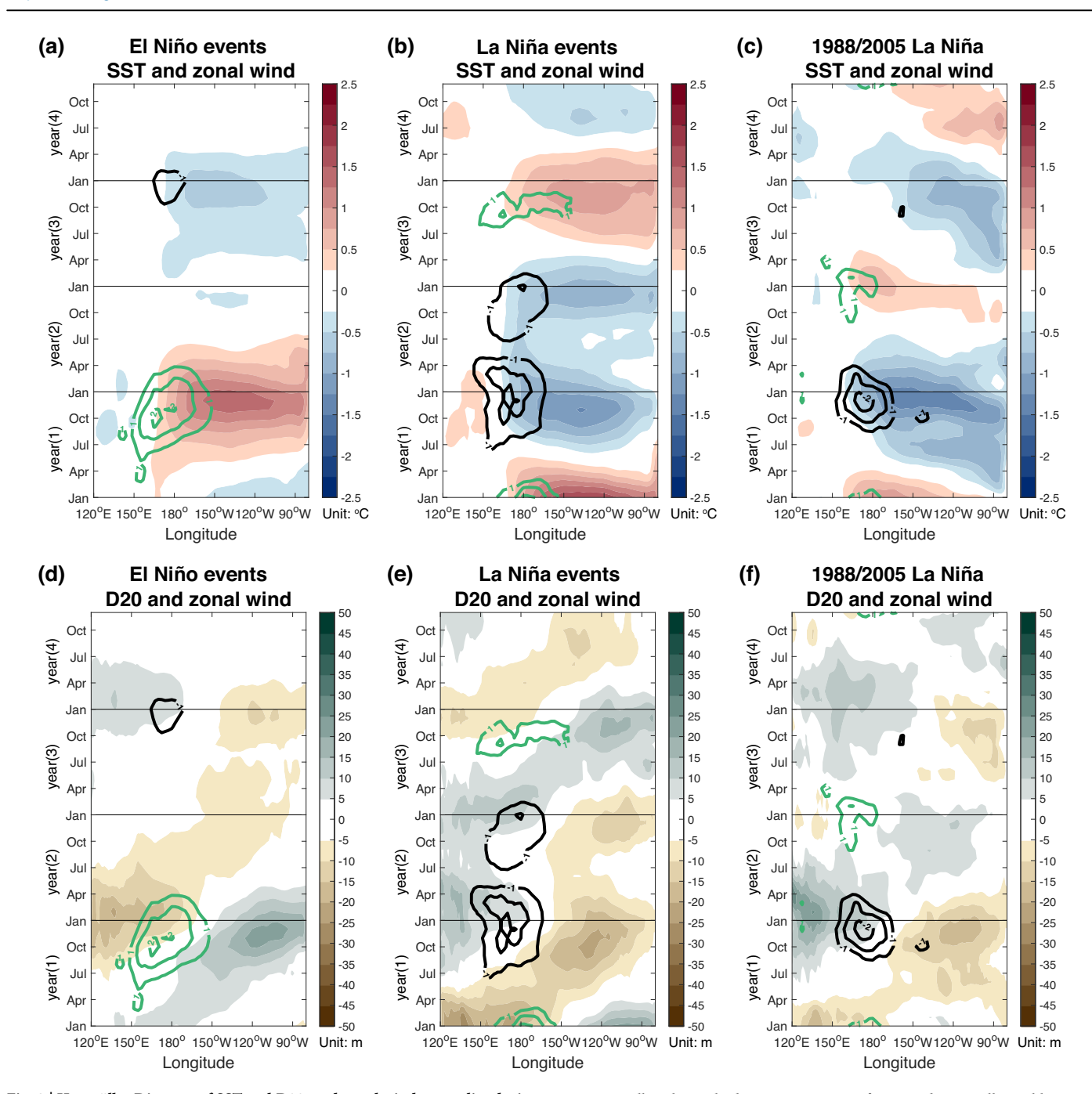


Fig. 3 | Hovmöller Diagram of SST and D20, and zonal wind anomalies during ENSO events. a-c SST anomalies (shaded) with zonal wind anomalies (contours) for El Niño events, La Niña events, and the 1988/2005 La Niña event, respectively. d-f D20 anomalies (shaded) with zonal wind anomalies (contours) for the same events. The La Niña events in (b) and (e) exclude the single-year events of 1988 and

2005, as well as the triple-dip La Niña events of 1998 and 2020. All variables are averaged between 5°S and 5°N. Green contours represent westerly wind anomalies, while black contours indicate easterly wind anomalies. The contour interval for wind anomalies is 0.5 m/s.

the equatorial Pacific. This robust linkage significantly contributed to the persistence of easterly anomalies, thereby prolonging the cold SSTA until the end of the third year.

In contrast to the 2020–2023 event, the 1998–2001 La Niña did not exhibit a significant anomalous meridional SLPA dipole associated with the SPMM during the second-year spring and summer (1999 MAM and JJA). Moreover, a reversed dipole pattern emerged in the third-year autumn (2000 SON), which was unfavorable for sustaining cold SSTA. This stark contrast highlights the distinct mechanisms driving the two triple-dip La Niña events: while the 1998–2001 event was primarily maintained by strong negative heat content anomalies and equatorial air-sea coupling, the

2020–2023 event relied heavily on persistent extratropical forcing, particularly from the Southern Hemisphere, to sustain equatorial easterly wind anomalies. These results underscore the critical role of both tropical ocean-atmosphere interactions and extratropical atmospheric variability in influencing the longevity and evolution of multi-year La Niña events.

# Prediction skill of EPM for 1998–2001 and 2020–2023 La Niña events

To further investigate the distinct driving mechanisms behind the 1998–2001 and 2020–2023 triple-dip La Niña events, we employ our physically based ENSO prediction model, EPM, to assess the relative

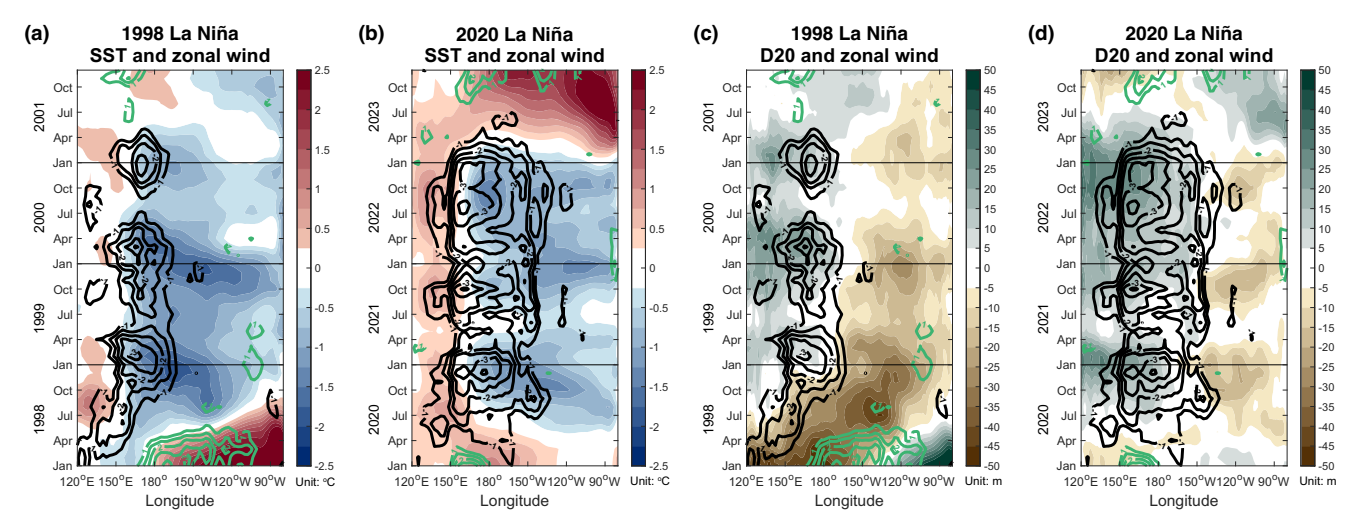


Fig. 4 | Hovmöller Diagram of SST and D20, and zonal wind anomalies during the triple-dip La Niña events. a, b SST anomalies (shaded) with zonal wind anomalies (contours) for 1998–2001 and 2020–2023 triple-dip La Niña events, respectively. c, d D20 anomalies (shaded) with zonal wind anomalies (contours) for

the same events. All variables are averaged between 5°S and 5°N. Green contours represent westerly wind anomalies, while black contours indicate easterly wind anomalies. The contour interval for wind anomalies is  $0.5 \, \text{m/s}$ .

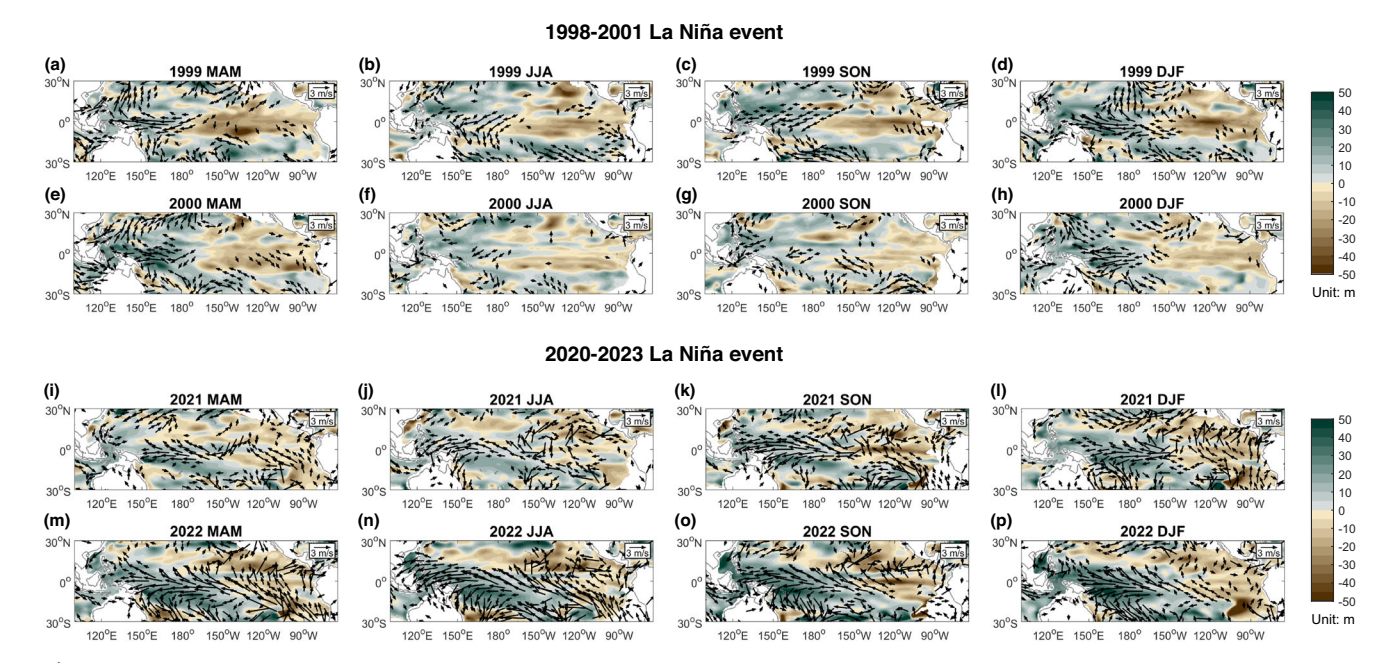


Fig. 5 | Spatial evolution of D20 and surface wind anomalies during the La Niña events of 1998–2001 and 2020–2023. The shading and vectors represent the D20 and surface wind anomalies for the second and third years of the  $(\mathbf{a}-\mathbf{h})$  1998–2001 and  $(\mathbf{i}-\mathbf{p})$ 

2020–2023 La Niña events, respectively. The scale and units of the vectors are shown in the top-right corner of the panel. Only wind speeds greater than 1 m/s are displayed.

contributions of different processes to these events. Figure 7 shows the predicted results along with their skill, measured by the root mean square error (RMSE) between observations and predictions. As discussed in Section "Evolution of 1998–2001 and 2020–2023 La Niña", the most notable difference influencing the persistence of cold SSTA between the 1998–2001 and 2020–2023 events occurred from spring to summer of the second- and third-year. Moreover, ENSO prediction during spring is particularly challenging, with lower prediction skills compared to other seasons, marking spring as a critical period for ENSO forecast. Therefore, we specifically focus on evaluating the model's prediction during this period (April and May in 1999/2000 and 2021/2022), with comprehensive results for other months are provided in Supplementary Figure 3. Here, we construct the EPM based on two configurations: the first, referred to as  $EPM_{TD+EX}$ , incorporates all predictors, including tropical ocean-atmosphere coupling and extratropical

processes ( $EP_{SST}$ ,  $EP_{WWV}$ ,  $EP_{OA}$ ,  $EP_{EX-N}$ , and  $EP_{EX-S}$ ), while the other, called  $EPM_{TD}$ , includes only tropical processes ( $EP_{SST}$ ,  $EP_{WWV}$ , and  $EP_{OA}$ ).

For the predictions starting from April and May of 1999 (Fig. 7a), the  $EPM_{TD}$  performs better for May (red dashed line) than for April (red solid line). This suggests that, despite favorable tropical Warm Water Volume (WWV) conditions conducive to La Niña development in April 1999 (Fig. 4c), there is an underestimation of La Niña's strength in the prediction, reflecting the well-documented challenge of ENSO prediction during the spring barrier. However, from May onwards, tropical ocean-atmosphere coupling conditions become more favorable for continued La Niña development. As a result, the  $EPM_{TD}$  produces predictions closer to the observations after the prediction from May 1999, although it still underestimates the amplitude of winter La Niña (Fig. 7a & Supplementary Fig. 3a). In contrast, the forecast errors for  $EPM_{TD+EX}$  predicted from May are higher

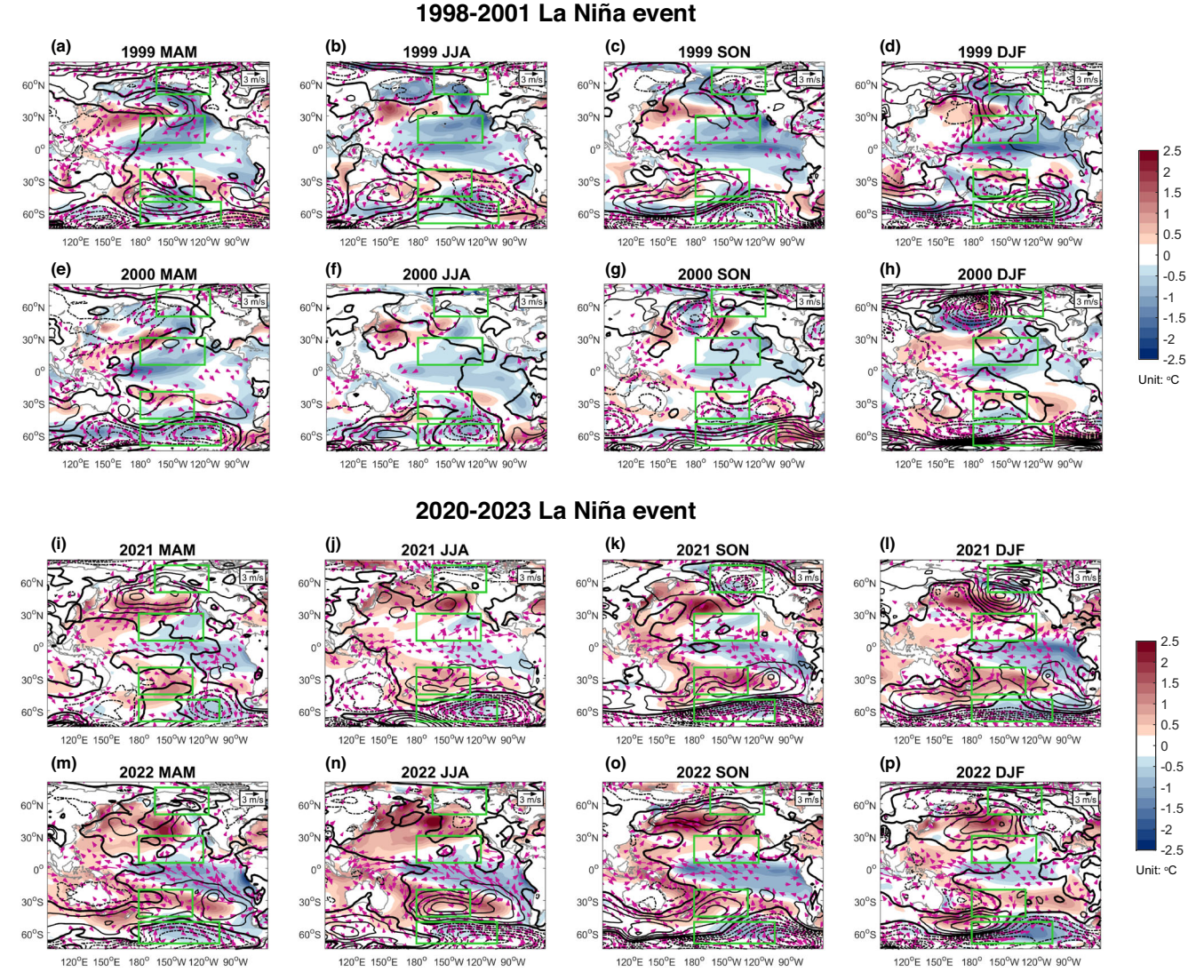


Fig. 6 | Spatial evolution of SST, SLP, and surface wind anomalies during the La Niña events of 1998–2001 and 2020–2023. The shading, contour lines, and vectors represent the SST, SLP, and surface wind anomalies for the second and third years of the (a-h) 1998–2001 and (i-p) 2020–2023 La Niña events, respectively. The contour interval for SLP anomalies is 1.5 hPa. The thick black contour indicates zero values,

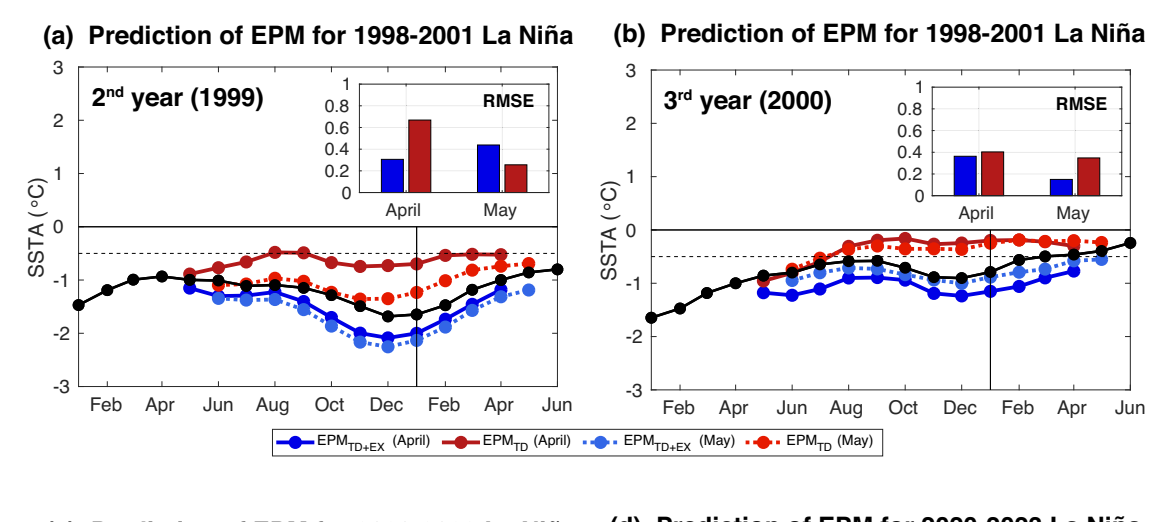
with solid and dashed contours representing positive and negative values, respectively. The scale and units of the vectors are shown in the top-right corner of the panel. Only wind speeds greater than 1 m/s are displayed. The four green boxes are used to define the extratropical precursor index as outlined in Section "ENSO prediction model".

than those for  $EPM_{TD}$  (RMSE shown in Fig. 7a), even though both April and May  $EPM_{TD+EX}$  forecasts indicate a strong La Niña in the following winter (solid and dashed blue lines in Fig. 7a, respectively). This indicates that the inclusion of extratropical forcing did not significantly improve ENSO prediction skills during late spring and early summer of 1999 (after May) due to the already favorable tropical ocean-atmosphere condition for La Niña development. However, in early spring (April), while tropical processes remain critical, incorporating extratropical processes significantly enhances prediction skills, highlighting their substantial contribution during this season<sup>29</sup>. On the other hand, for the predictions starting from April and May of 2000 (Fig. 7b), the  $EPM_{TD}$  (red lines) fails to predict the subsequent La Niña event in winter. This might be attributed to weakened WWV as La Niña entered its third year (Fig. 4c). However, when extratropical forcing is included in EPM<sub>TD+EX</sub> (blue lines), prediction skill improves, suggesting that extratropical signals play a role in sustaining La Niña conditions in the third year of this event.

For the predictions starting from April and May of 2021 (Fig. 7c), the  $EPM_{TD}$  fails to accurately forecast the La Niña event. In contrast, the  $EPM_{TD+EX}$  model successfully predicts the occurrence of the upcoming La Niña event (solid and dashed blue lines). This improvement can be

attributed to the distinct characteristics of the 2020–2023 La Niña, which was marked by relatively weak negative heat content anomalies. Under these conditions, the tropical-only model ( $EPM_{TD}$ ) struggled to predict La Niña effectively, while extratropical forcing—especially from the Southern Hemisphere—provided persistent equatorial easterly wind anomalies that sustained cold SSTA (Fig. 6). By accounting for these extratropical influences, the  $EPM_{TD+EX}$  successfully predicted the 2021 La Niña event in spring. Meanwhile, for the 2022 predictions (Fig. 7d),  $EPM_{TD}$  forecasts starting in both April and May exhibited poor performance prior to winter, although the May-started forecast was better able to capture the La Niña amplitude during the winter. Including extratropical forcing in  $EPM_{TD+EX}$  improved the prediction before winter, but it tended to overestimate La Niña's amplitude during winter, which may be attributed to the fact that the peak of observed SSTA did not occur in the winter season.

Overall, for the second year of 1998–2001 La Niña event, the model considering only tropical processes successfully predicted La Niña development, as tropical ocean-atmosphere coupling remained favorable. However, when the heat content decreased in the third year, it become necessary to incorporate extratropical forcing to better predict La Niña's SSTA, particularly in capturing SST variations. In contrast, for the



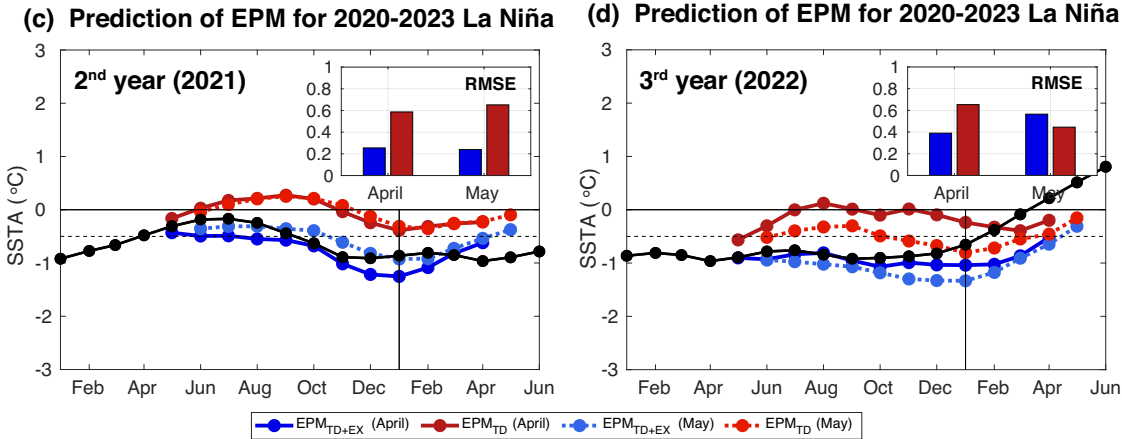


Fig. 7 | Predictions of EPM for 1998–2001 and 2020–2023 La Niña events. ENSO predicted results and their skill by EPM starting from April and May of (a) 1999, (b) 2000, (c) 2021, and (d) 2022. The black lines are the observations. The blue and red lines represent the predicted values by  $EPM_{TD+EX}$  and  $EPM_{TD}$ , respectively. Solid

lines show predictions starting from April, while dashed lines indicate predictions starting from May. The prediction skill is quantified by the RMSE between observations and predictions, as shown in the top right of each panel.

2020–2023 event, the lack of sufficient negative heat content anomalies throughout the period limited the prediction skill of the tropical-only model. Under these conditions, incorporating extratropical forcing significantly improved prediction by sustaining equatorial easterly wind anomalies that supported cold SSTA. These results highlight the importance of considering extratropical processes in ENSO prediction, especially for events with atypical tropical ocean conditions, such as the 2020–2023 La Niña.

### Individual contributions of predictors in the EPM

To better understand the role of individual predictors in ENSO forecasts, Fig. 8 illustrates the relative contributions of different ENSO predictors in the EPM for the years 1999/2000 and 2021/2022. Additionally, Supplementary Figure 4 presents the combined effects of all predictors ( $EP_{SST}$ ,  $EP_{WWV}$ ,  $EP_{OA}$ ,  $EP_{EX-N}$ , and  $EP_{EX-S}$ ), as well as the contributions tropical ocean-atmosphere coupling processes ( $EP_{SST}$ ,  $EP_{WWV}$ , and  $EP_{OA}$ ) and extratropical processes ( $EP_{EX-N}$  and  $EP_{EX-S}$ ). In each panel, the x-axis represents the lead month for forecasting, while the y-axis shows the starting calendar month. The combined effect of all predictors (Supplementary Fig. 4a, d, g, j) reveals strong cold SSTA contributions across most predicted months in both 1999/2000 and 2021/2022, indicating a robust signal for the second- and third-year La Niña development.

Among all predictors, the  $EP_{SST}$  exhibits a significant contribution to the cold SSTA after late spring in both 1999/2000 and 2021/2022 (Fig. 8a, f, k, p), emphasizing the importance of SSTA persistence in the ENSO forecast. Regarding  $EP_{WWV}$ , in 1999 (Fig. 8b), the contributions from equatorial propagating WWV show strong cold SSTA contributions before July,

suggesting that  $EP_{WWV}$  plays an important role in spring and early summer in maintaining the cold SSTA for the second-year of 1998-2001 La Niña. This is consistent with previous findings that, in the 1998-2001 triple-dip La Niña event, sufficient cold anomalies in heat content, generated by a significant discharge process, helped sustain subsequent La Niña events<sup>32</sup>. However, *EP*<sub>WWV</sub> in 2000 (Fig. 8g), the third year of the 1998–2001 La Niña, showed only small cold SSTA contributions before June and shifted to warm SSTA contributions afterward. This reflects the decreased negative heat content anomalies during this period, as discussed in Section "Prediction skill of EPM for 1998-2001 and 2020-2023 La Niña events". For the 2020–2023 La Niña event,  $EP_{WWV}$  in 2021 (Fig. 8l) provides a warm SSTA contribution from May to August, while  $EP_{WWV}$  in 2022 (Fig. 8q) contributes to warm SSTA almost throughout the entire year. This suggests that WWV conditions in 2021/2022 were not favorable for maintaining La Niña into the following year and instead tended to promote the decay of cold SSTA.

The  $EP_{OA}$  predictor (Fig. 8c, h, m, r), which represents the ocean-atmosphere feedback, contributes to cold SSTA development during the early summer of both 1999/2000 and 2021/2022. This occurs because summer is the most unstable season for equatorial Pacific SSTA, characterized by a larger SSTA growth rate with the most significant wind-induced coupling processes during this time<sup>33,38</sup>. Next, we examine the individual contributions of extratropical forcing from the Northern and Southern Hemispheres ( $EP_{EX-N}$  and  $EP_{EX-S}$ , respectively). In 1999/2000, the Northern Hemisphere contribution is more significant (Fig. 8d, i) compared to the Southern Hemisphere contribution (Fig. 8e, j), with the

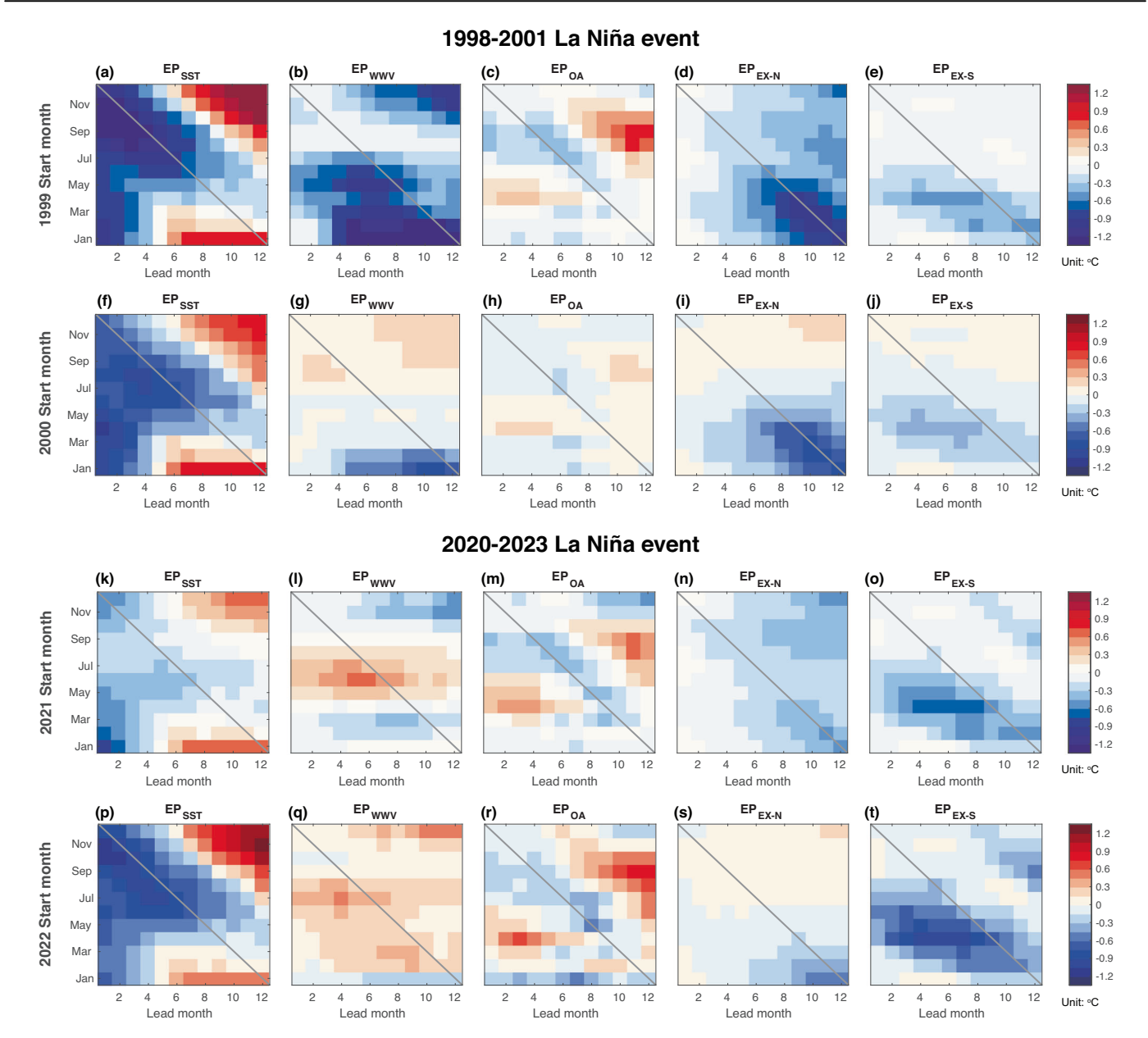


Fig. 8 | Contribution of different processes to predicted SSTA in EPM for 1998–2001 and 2020–2023 La Niña events. The panels show the contribution of SSTA  $(EP_{SST})$ , WWV propagation  $(EP_{WWV})$ , the tropical ocean-atmosphere feedback  $(EP_{OA})$ , and the extratropical forcing from the Northern  $(EP_{EX-N})$  and

Southern Hemispheres ( $EP_{EX-S}$ ) to predicted SSTA for ( $\mathbf{a}$ - $\mathbf{e}$ ) 1999, ( $\mathbf{f}$ - $\mathbf{j}$ ) 2000, ( $\mathbf{k}$ - $\mathbf{o}$ ) 2021, and ( $\mathbf{p}$ - $\mathbf{t}$ ) 2022. The x-axis for each panel represents the lead month for predicting, and the y-axis indicates the start calendar month. Grey lines indicate the predicted SSTA for December.

primary impact observed in the predicted winter SSTA. In contrast, for 2021/2022, the Southern Hemisphere's contribution is more substantial during spring start months (Fig. 8o, t), also affecting the predicted winter SSTA. These findings are consistent with previous conclusions: in 2021/2022, the extratropical forcing from the Southern Hemisphere was strong, sustaining persistent easterly winds along the equator and supporting the continuation of cold SSTA.

Summing up all the contributions from tropical processes and comparing them to those from extratropical processes (Supplementary Fig. 4), we find that in 1999, considering only tropical processes is sufficient to forecast the subsequent cold SSTA (Supplementary Fig. 4b). However, in 2000, due to the weak cold SSTA contribution from  $EP_{WWV}$ , relying solely on tropical processes is insufficient to predict the subsequent La Niña event, as the SSTA does not fall below  $-0.5\,^{\circ}\mathrm{C}$  when forecast starts from spring (Supplementary Fig. 4e). For the 2020–2023 La Niña event, tropical dynamics alone are not enough to successfully predict the La Niña event

during spring of 2021/2022 and even result in the erroneously warm SSTA in 2022 (Supplementary Fig. 4h and k). Accurate forecasting can only be achieved by incorporating extratropical processes (Supplementary Fig. 4i and l). These results indicate that the EPM effectively captures the distinct driving mechanisms behind the two triple-dip La Niña events. For the 1998–2001 event, tropical processes dominated the prediction skill, especially during the second year, while for the 2020–2023 event, extratropical forcing significantly enhanced forecast accuracy.

#### **Discussion**

This study investigates the mechanisms driving consecutive La Niña events using a physically based EPM from a prediction perspective. The results confirm distinct driving mechanisms behind the 1998–2001 and 2020–2023 triple-dip La Niña events. The 1998–2001 event was primarily sustained by substantial negative heat content anomalies in the equatorial Pacific, a consequence of the strong El Niño discharge process preceding it. Tropical

predictors, such as SSTA, WWV propagation, and ocean-atmosphere feedback, played a dominant role in prediction skill, particularly in the second year. Meanwhile, extratropical forcing from the North Pacific also contributed to the persistence of cold SSTA. However, as the event progressed into the third year, the diminishing negative heat content anomalies reduced the effectiveness of tropical processes along in sustaining cold SSTA. At this stage, extratropical forcing became more influential, enhancing the model's ability to predict SST variations. In contrast, the 2020-2023 La Niña event presented different characteristics of prediction based on the EPM results. Due to the absence of significant negative heat content anomalies throughout the event, the tropical-only EPM struggled to accurately forecast the La Niña development, particularly in the second and third years. This is why most models in the IRI/CPC ENSO plume fail to correctly forecast the second year La Niña. Incorporating extratropical forcing significantly improved the prediction skill, especially by better capturing the persistent equatorial easterly wind anomalies, which were sustained by strong extratropical signals from the Southern Hemisphere.

These results highlight the importance of extratropical influences in ENSO prediction. While tropical ocean-atmosphere coupling remains the dominant driver when heat content anomalies are strong, extratropical forcing becomes essential under conditions of weakened tropical heat content<sup>25,27</sup>, as observed in the third year of the 1998-2001 event and throughout the 2020-2023 event. Kim et al. (2023) also noted that over half of multi-year La Niña events do not require a preceding strong El Niño but are instead associated with a negative NPMM during the decay spring of the first event<sup>22</sup>. Given the increased influence of extratropical forcing under global warming<sup>39</sup>, the frequency of such events is expected to rise in the future, making it increasingly important to account for these influences to enhance the accuracy of climate models and ENSO forecast. However, incorporating extratropical forcing may lead to an overestimation of La Niña amplitude in EPM predictions, as discussed in Section "Prediction skill of EPM for 1998-2001 and 2020-2023 La Niña events". To better improve future prediction, more emphasis should be placed on investigating the contribution of extratropical forcing to the model's amplitude of ENSOrelated SSTA and exploring how these processes might be modulated by climate change. A deeper understanding of these dynamics is critical for enhancing the predictability of multi-year La Niña events under future climate scenarios.

Regarding the driving mechanisms of the 1998–2001 and 2020–2023 triple-dip La Niña events, in addition to the ocean heat content and extratropical forcing from the Southern Hemisphere highlighted in this study, other studies have also proposed additional mechanisms. Iwakiri et al. (2023) identified a critical role of North Pacific high-pressure anomalies during the winter of 2020/2021, which induced a negative NPMM in the following spring<sup>40</sup>. While our study also references the NPMM phenomenon, Iwakiri et al. (2023) emphasizes that the meridional extent of the La Niña SSTA pattern can slow down the recharge-discharge process, contributing to the development of a second-year La Niña. In addition, Li et al. (2023) documented that changes in the mean state of the tropical Pacific, characterized by an increased zonal SST gradient and strengthened trade winds, associated with the ENSO regime shift around 1999/2000<sup>41-43</sup>, played a crucial role in the development of the 2020-2023 La Niña and contributed to improved prediction skill<sup>32</sup>. They also indicated that the dominant feedback mechanisms differed between the two events, with thermocline feedback playing a key role in the 1998-2001 La Niña, while zonal advection feedback was more prominent during the 2020-2023 La Niña.

Interestingly, Li et al. (2023) found that the North American Multi-Model Ensemble (NMME) models exhibited higher prediction skills for the 2020–2023 La Niña compared to the 1998–2001 event<sup>32</sup>. This result contradicts our intuition, as the traditional recharge-discharge framework suggests that strong (weak) discharge implies high (low) predictability of multiyear La Niña<sup>44,45</sup>. They argue that even without sufficient equatorial Pacific negative heat content, the La Niña-like mean state of the equatorial Pacific contributed to the predictability of the 2020-2023 triple-dip La Niña. We note that better prediction skill for the 2020-2023 La Niña in Li et al. (2023) comes from extremely larger model biases in the first-year prediction of the 1998-2001 La Niña (their Fig. 9). If comparing only the second- and thirdyear events, their results will be consistent to our results. Indeed, most prediction models in the IRI/CPC ENSO plume struggled to accurately predict the second-year La Niña during the spring of 2021 (Fig. 2). While NMME models performed relatively well in predicting the second-year La Niña of the 2020-2023 event from April 2021, the performance of most models in the International Multi-Model Ensemble (IMME) was not as good, as they predicted September SSTA values that did not below -0.5 °C (https://www. cpc.ncep.noaa.gov/products/NMME/archive/2021040800/current/plume. html). This suggests that discrepancies among different models and initialization data play a significant role in the predictability of multi-year La Niña events. Since the IRI/CPC ENSO plume only began in 2002, a direct comparison of predictability between the 1998-2001 and 2020-2023 multi-year La Niña events is not possible. Therefore, we do not attempt to determine which triple-dip La Niña event had higher prediction skill across ENSO prediction models, which is beyond the scope of this study.

#### Methods

#### Observation data and ENSO definition

The observational SST used in analysis is obtained from the monthly  $2^{\circ} \times 2^{\circ}$  NOAA Extended Reconstructed Sea Surface Temperature version 5 (ERSSTv5)<sup>46</sup>. The thermocline depth is defined as the depth of 20 °C isotherm (D20) and is estimated using the monthly  $1/3^{\circ} \times 1.0^{\circ}$  global ocean data assimilation system (GODAS)<sup>47</sup>. The monthly near-surface wind data (0.995-sigma level) and sea-level pressure data are from the National Centers for Environmental Prediction and National Center for Atmospheric Research (NCEP-NCAR) reanalysis project<sup>48</sup>, with a horizontal grid resolution of 2.5° × 2.5°. All datasets cover the period from 1980 to 2023 and anomalies were calculated relative to the climatology of this same period.

ENSO evolution is characterized by the Niño34 index, which is the SSTA averaged over the region bounded by 5°N-5°S, 170°W-120°W in the equatorial Pacific. ENSO events are defined based on the 3-month running average of the Niño 3.4 index. Anomalies at or above +0.5 °C for 5 consecutive months are El Niño events and anomalies below -0.5 °C for 5 consecutive months are La Niña events. The list of ENSO events is shown in Table 1.

### **ENSO** prediction model

A physical-based statistical ENSO prediction model, EPM, is utilized in this study to investigate the trigger mechanism of triple-dip La Niña events and their predictability. The EPM is established as follows:

$$\begin{split} EPM\big(m+\varphi\big) &= \frac{\sigma_O(m,\varphi)}{\sigma_P(m,\varphi)} [\beta_1\big(m,\varphi\big) EP_{SST}(m) + \beta_2\big(m,\varphi\big) EP_{WWV}(m) + \beta_3\big(m,\varphi\big) EP_{OA}(m) \\ &+ \beta_4\big(m,\varphi\big) EP_{EX-N}(m) + \beta_5\big(m,\varphi\big) EP_{EX-S}(m)] \end{split}$$

(1)

# Table 1 | List of El Niño and La Niña events

	Years
El Niño	1982–1983, 1986–1988*, 1991–1992, 1994–1995, 1997–1998, 2002–2003, 2004–2005, 2006–2007, 2009–2010, 2014–2016*, 2018–2019
La Niña	1983–1985*, 1988–1989, 1995–1996, 1998–2001*, 2005–06, 2007–2009*, 2010–2012*, 2016–2018*, 2020–2023*

The superscript \* and # indicate the double-dip and triple-dip events, respectively, while unmarked events are single-year events. Note that although the 1995–1996 event is categorized as a single La Niña event, the value for the second-year winter is very close to the event thresholds.

Considering the physical dynamics associated with tropical ocean-atmosphere coupling and extratropical processes, this EPM consists of five ENSO predictors: the ENSO SSTA in the Niño34 region ( $EP_{SST}$ ), the WWV propagation in the central Pacific ( $EP_{WWV}$ ), the tropical ocean-atmosphere feedback ( $EP_{OA}$ ), and the extratropical forcing from the Northern ( $EP_{EX-N}$ ) and Southern Hemispheres ( $EP_{EX-S}$ ). The  $EP_{SST}$  is estimated as the SSTA averaged over the Niño34 region. The  $EP_{WWV}$  is defined as the equatorial D20 anomalies (averaged between 2°S and 2°N) at 180°, 170°W, and 155°W over different times to reflect the eastern propagation feature of WWV. The  $EP_{OA}$  is determined by the time-accumulated zonal surface wind anomalies across the equatorial central Pacific region (180°-170°W and 2°S-2°N). The  $EP_{EX-N}$  and  $EP_{EX-S}$  consider the dipole pattern of SLPA in the Northern and Southern Hemispheres as follows:

$$EP_{EX-N} = SLPA_{N1} - SLPA_{N2} \tag{2}$$

$$EP_{EX-S} = SLPA_{S2} - SLPA_{S1} \tag{3}$$

The four key regions for SLPA are defined as follows: N1 (165°-115°W, 50°-75°N), N2 (180°-120°W, 5°-30°N), S1 (180°-130°W, 20°-45°S), and S2 (180°–105°W, 50°–70°S). The predictor  $EP_{SST}$  is calculated from monthly data and the predictors  $EP_{WWV}$ ,  $EP_{OA}$ ,  $EP_{EX-N}$ , and  $EP_{EX-S}$  are calculated from the pentad data and subsequently averaged to monthly data with standardization. The coefficients of the predictors  $(\beta_1, \beta_2, \beta_3, \beta_4 \text{ and } \beta_5)$  for forecast lead times  $(\varphi)$  with different start calendar months (m) are determined through multivariate linear regression. To better match the seasonal variance of observations, the monthly scaling function  $\frac{\sigma_O(m,\varphi)}{\sigma_P(m,\varphi)}$  is used to normalize the prediction, where  $\sigma_O$  and  $\sigma_P$  are the standard deviations of the ENSO index for the observations and prediction, respectively, in the different start calendar months and lead-time. To ensure consistency with the predictions provided to the IRI/CPC ENSO plume, the dataset used for the ENSO prediction model in this study differs from that used in the analysis. The monthly Niño34 index for EP<sub>SST</sub> is provide by the CPC, which is estimated based on the Optimum Interpolation SST version 2.1  $(OISSTv2.1)^{49}$ ; The pentad D20 data for calculating  $EP_{WWV}$  are from GODAS, while the pentad surface zonal wind for  $EP_{OA}$  and pentad SLP data for  $EP_{EX-N}$  and  $EP_{EX-S}$  are derived from the NCEP-NCAR reanalysis. Detailed definitions of EPM can be found in Supplementary Text 1.

Our EPM is a physical-based statistical model that captures not only the dynamics of ENSO evolution within the recharge-discharge oscillation framework<sup>19</sup> but also reflects the influence of extratropical forcing beyond the spring predictability barrier<sup>29,30</sup>. The predictors of EPM are independent and contribute differently at various lead-times<sup>30</sup>. According to the evaluation by Chen et al. (2020)<sup>29</sup>, the EPM demonstrates strong prediction skill for ENSO events, with correlation scores of 0.70, 0.65, and 0.61 for lead times of 6, 8, and 10 months, respectively, based on monthly mean Niño34 index. The percentage correct metric for 1980-2020 indicates that, with a 6-month lead, the EPM achieved 92% accuracy for El Niño and 86% for La Niña. Additionally, the EPM successfully predicted the most recent 2024-2025 La Niña condition from April 2024 (Supplementary Fig. 5). Moreover, it was one of only three forecasting models in the IRI/CPC ENSO plume that successfully predicted the occurrence of the multi-year La Niña in April 2021 for the 2021-2022 event (Fig. 2; https://iri.columbia.edu/ourexpertise/climate/forecasts/enso/2021-April-quick-look/). These results demonstrate the robustness of EPM in capturing most ENSO events, suggesting that it is a valuable tool for exploring and validating the dynamical mechanisms and predictability of consecutive La Niña events in this study.

# **Data availability**

The datasets used in this study are available through the following websites: ERSSTv5 at https://psl.noaa.gov/data/gridded/data.noaa.ersst.v5. html; GODAS at https://www.psl.noaa.gov/data/gridded/data.godas.html; NCEP-NCAR reanalysis at https://psl.noaa.gov/data/gridded/data.ncep. reanalysis.html; Niño34 index used in the EPM is provided by the CPC

and can be accessed at https://www.cpc.ncep.noaa.gov/data/indices/. **EPM forecast data** can be found at https://iri.columbia.edu/our-expertise/climate/forecasts/enso/current/?enso\_tab=enso-sst\_table, provided by IRI for Climate and Society, Columbia University Climate School (https://iri.columbia.edu/ENSO), or can request IRI's ENSO archive data at https://docs.google.com/forms/d/e/1FAIpQLSf2WoM0nV\_D5xppn7wPMQrQw23VPLNBnK O2ycpFFe8J8dia-A/viewform.

# Code availability

The source codes for the analysis of this study can be requested from the first author

Received: 27 August 2024; Accepted: 12 March 2025; Published online: 16 April 2025

#### References

- Cole, J. E., Overpeck, J. T. & Cook, E. R. Multiyear La Niña events and persistent drought in the contiguous United States. *Geophys. Res. Lett.* 29, 25–1 (2002).
- Okumura, Y. M., DiNezio, P. & Deser, C. Evolving impacts of multiyear La Niña events on atmospheric circulation and U.S. drought. Geophys. Res. Lett. 44, 11,614–11,623 (2017).
- Iwakiri, T. & Watanabe, M. Multiyear La Niña impact on summer temperature over Japan. J. Meteorol. Soc. Jpn. Ser. II 98, 1245–1260 (2020).
- Luo, J. J., Liu, G., Hendon, H., Alves, O. & Yamagata, T. Inter-basin sources for two-year predictability of the multi-year La Niña event in 2010–2012. Sci. Rep. 7, 1–7 (2017).
- Wang, B. et al. Understanding the recent increase in multiyear La Niñas. Nat. Clim. Change 13, 1075–1081 (2023).
- Yu, J. Y. & Fang, S. W. The distinct contributions of the seasonal footprinting and charged-discharged mechanisms to ENSO Complexity. *Geophys. Res. Lett.* 45, 6611–6618 (2018).
- Ding, R. et al. Multi-year El Niño events tied to the North Pacific Oscillation. Nat. Commun. 13, 1–11 (2022).
- Park, J. H. et al. Mid-latitude leading double-dip La Niña. Int. J. Climatol. 41, E1353–E1370 (2021).
- 9. Song, C., Zhang, X., Zheng, F., Chen, X. & Jiang, H. The roles of off-equatorial subsurface cold-water incursions in triggering the second-year cooling of the La Niña event in 2021. *J. Mar. Sci. Eng.* **10**, 1667 (2022).
- Fang, X. et al. Will the historic southeasterly wind over the Equatorial Pacific in March 2022 trigger a third-year La Niña event? Adv. Atmos. Sci. 40, 6–13 (2023).
- Iwakiri, T. & Watanabe, M. Mechanisms linking multi-year La Niña with preceding strong El Niño. Sci. Rep. 11, 17465 (2021).
- 12. Wu, X., Okumura, Y. M. & Dinezio, P. N. What controls the duration of El Niño and La Niña Events? *J. Clim.* **32**, 5941–5965 (2019).
- 13. Hu, Z. Z., Kumar, A., Xue, Y. & Jha, B. Why were some La Niñas followed by another La Niña? Clim. Dyn. 42, 1029–1042 (2014).
- Lengaigne, M., Boulanger, J.-P., Menkes, C. & Spencer, H. Influence of the seasonal cycle on the termination of El Niño events in a coupled general circulation model. *J. Clim.* 19, 1850–1868 (2006).
- Iwakiri, T. & Watanabe, M. Multiyear ENSO dynamics as revealed in observations, climate model simulations, and the linear recharge oscillator. J. Clim. 35, 7625–7642 (2022).
- Zhang, W., Li, J. & Jin, F. F. Spatial and temporal features of ENSO meridional scales. *Geophys. Res. Lett.* 36, 15605 (2009).
- Gao, Z. et al. Single-year and double-year El Niños. Clim. Dyn. 60, 2235–2243 (2023).
- Vimont, D. J., Battisti, D. S. & Hirst, A. C. The seasonal footprinting mechanism in the CSIRO general circulation models. *J. Clim.* 16, 2653–2667 (2003).
- Jin, F.-F. An equatorial ocean recharge paradigm for ENSO. Part I: conceptual model. J. Atmos. Sci. 54, 811–829 (1997).

- Chiang, J. C. H. & Vimont, D. J. Analogous Pacific and Atlantic meridional modes of tropical atmosphere-ocean variability. *J. Clim.* 17, 4143–4158 (2004).
- Dong, X., Zhang, R.-H., Hu, J., Gao, C. & Chen, M. Thermodynamic processes prolong triple La Niña events in a hybrid coupled oceanatmosphere model. Clim. Dyn. 63, 1–16 (2025).
- 22. Kim, J. W., Yu, J. Y. & Tian, B. Overemphasized role of preceding strong El Niño in generating multi-year La Niña events. *Nat. Commun.* **14**, 1–11 (2023).
- Kim, J. W. & Yu, J. Y. Single- and multi-year ENSO events controlled by pantropical climate interactions. NPJ Clim. Atmos. Sci. 5, 1–11 (2022).
- Fan, H., Wang, C. & Yang, S. Asymmetry between positive and negative phases of the Pacific meridional mode: a contributor to ENSO transition complexity. *Geophys. Res. Lett.* 50, e2023GL104000 (2023).
- Zhao, S. et al. Explainable El Niño predictability from climate mode interactions. *Nature* 630, 891–898 (2024).
- Iwakiri, T. et al. Triple-Dip La Niña in 2020–23: North Pacific Atmosphere Drives 2nd Year La Niña. Geophys. Res. Lett 50, e2023GL105763 (2023).
- Shi, L., Ding, R., Hu, S., Li, X. & Li, J. Extratropical impacts on the 2020–2023 Triple-Dip La Niña event. *Atmos. Res.* 294, 106937 (2023).
- Zhang, H., Clement, A. & Di Nezio, P. The South Pacific Meridional Mode: a mechanism for ENSO-like variability. *J. Clim.* 27, 769–783 (2013).
- Chen, H. C., Tseng, Y. H., Hu, Z. Z. & Ding, R. Enhancing the ENSO predictability beyond the Spring Barrier. Sci. Rep. 10, 1–12 (2020).
- Tseng, Y. H., Huang, J. H. & Chen, H. C. Improving the predictability of two types of ENSO by the characteristics of extratropical precursors. *Geophys. Res. Lett.* 49, e2021GL097190 (2022).
- Tseng, Y. H., Hu, Z. Z., Ding, R. & Chen, H. C. An ENSO prediction approach based on ocean conditions and ocean–atmosphere coupling. *Clim. Dyn.* 48, 2025–2044 (2017).
- Li, X., Hu, Z. Z., McPhaden, M. J., Zhu, C. & Liu, Y. Triple-Dip La Niñas in 1998–2001 and 2020–2023: impact of mean state changes. *J. Geophys. Res. Atmos.* 128, e2023JD038843 (2023).
- 33. Li, T. Phase transition of the El Niño–Southern Oscillation: a stationary SST mode. *J. Atmos. Sci.* **54**, 2872–2887 (1997).
- 34. Chakravorty, S. et al. Testing the trade wind charging mechanism and its influence on ENSO variability. *J. Clim.* **33**, 7391–7411 (2020).
- Anderson, B. T. & Perez, R. C. ENSO and non-ENSO induced charging and discharging of the equatorial Pacific. *Clim. Dyn.* 45, 2309–2327 (2015).
- Anderson, B. T., Perez, R. C. & Karspeck, A. Triggering of El Niño onset through trade wind-induced charging of the equatorial Pacific. Geophys Res Lett. 40, 1212–1216 (2013).
- Anderson, B. T. Intraseasonal atmospheric variability in the extratropics and its relation to the onset of tropical Pacific sea surface temperature anomalies. *J. Clim.* 20, 926–936 (2007).
- 38. Chen, H. & Jin, F. Dynamics of ENSO phase–locking and its biases in climate models. *Geophys. Res. Lett.* **49**, 1–11 (2022).
- Liguori, G. & Di Lorenzo, E. Meridional modes and increasing pacific decadal variability under anthropogenic forcing. *Geophys. Res. Lett.* 45, 983–991 (2018).
- Iwakiri, T. et al. Triple-Dip La Niña in 2020–23: North Pacific atmosphere drives 2nd Year La Niña. Geophys. Res. Lett. 50, e2023GL105763 (2023).
- Hu, Z.-Z. et al. Weakened interannual variability in the Tropical Pacific Ocean since 2000. J. Clim. 26, 2601–2613 (2012).
- Hu, Z. Z. et al. The Interdecadal Shift of ENSO Properties in 1999/ 2000: a review. J. Clim. 33, 4441–4462 (2020).
- 43. McPhaden, M. J. A 21st century shift in the relationship between ENSO SST and warm water volume anomalies. *Geophys. Res. Lett.* **39**, (2012).

- Wu, X., Okumura, Y. M., Deser, C. & Dinezio, P. N. Two-year dynamical predictions of ENSO event duration during 1954–2015. *J. Clim.* 34, 4069–4087 (2021).
- DiNezio, P. N., Deser, C., Okumura, Y. & Karspeck, A. Predictability of 2-year La Niña events in a coupled general circulation model. *Clim. Dyn.* 49, 4237–4261 (2017).
- Huang, B. et al. Extended reconstructed sea surface temperature, version 5 (ERSSTv5): upgrades, validations, and intercomparisons. *J. Clim.* 30, 8179–8205 (2017).
- Behringer, D. W. & Xue, Y. Evaluation of the Global Ocean Data Assimilation System at NCEP: The Pacific Ocean. in 11–15 (American Meteorological Society, 2004).
- 48. Kalnay, E. et al. The NCEP/NCAR 40-year reanalysis project. *Bull. Am. Meteorol. Soc.* 77, 437–472 (1996).
- Huang, B. et al. Improvements of the Daily Optimum Interpolation Sea Surface Temperature (DOISST) Version 2.1. J. Clim. 34, 2923–2939 (2021).

# **Acknowledgements**

H.-C. Chen was supported by NSFC project 42205022 and project JSSCTD202346. Y.-H. Tseng was supported by NSTC Grant#112-2611-M-002-016-MY3.

#### **Author contributions**

H.-C. Chen and Y.-H. Tseng developed the idea and wrote the study. H.-C. Chen, J.-H. Huang, and P.-H. Juang performed the research and analyzed the data.

### Competing interests

The authors declare no competing interests.

#### Additional information

**Supplementary information** The online version contains supplementary material available at https://doi.org/10.1038/s41612-025-01004-0.

**Correspondence** and requests for materials should be addressed to Han-Ching Chen or Yu-Heng Tseng.

**Reprints and permissions information** is available at http://www.nature.com/reprints

**Publisher's note** Springer Nature remains neutral with regard to jurisdictional claims in published maps and institutional affiliations.

Open Access This article is licensed under a Creative Commons Attribution-NonCommercial-NoDerivatives 4.0 International License, which permits any non-commercial use, sharing, distribution and reproduction in any medium or format, as long as you give appropriate credit to the original author(s) and the source, provide a link to the Creative Commons licence, and indicate if you modified the licensed material. You do not have permission under this licence to share adapted material derived from this article or parts of it. The images or other third party material in this article are included in the article's Creative Commons licence, unless indicated otherwise in a credit line to the material. If material is not included in the article's Creative Commons licence and your intended use is not permitted by statutory regulation or exceeds the permitted use, you will need to obtain permission directly from the copyright holder. To view a copy of this licence, visit http://creativecommons.org/licenses/by-nc-nd/4.0/.

© The Author(s) 2025